



## Fabrication of Amniotic Membrane coated Silk Fibroin nanofibers Containing Thymol for Antibacterial Wound Dressing

Parisa Akhlaghi<sup>1</sup>, Rouhollah Mehdinavaz Aghdam<sup>\*1</sup>, Sina Ashouri Sharafshadeh<sup>1</sup>, Yalda Pirhadi  
Tavandashi<sup>1</sup>

<sup>1</sup>Biomaterials Lab, School of Metallurgy and Materials Engineering, College of Engineering, University of  
Tehran, P.O. Box: 11155-4563, Tehran, Iran.

Received: 16 October 2024; Accepted: 24 April 2025

\*Corresponding author, E-mail: [mehdinavaz@ut.ac.ir](mailto:mehdinavaz@ut.ac.ir)

### ABSTRACT

Bacterial wound infection delays wound healing and may lead to life-threatening complications. Hence wound dressing materials are not restricted to stop blood loss, but also to protect the wound from bacterial infection and to accelerate the wound healing process. In this study, biopolymeric nanofibers of Silk Fibroin (SF) and decellularized human Amniotic membrane (dehAM) were fabricated by electrospinning technique to be used in wound healing. Thymol, a natural antibacterial substance, solutions containing 5% wt/wt, 10%wt/wt and 15% wt/wt thymol was added to the SF nanofibers to increase the sustained release. Scanning Electron Microscopy and Attenuated Total Reflectance Fourier-Transform Infrared (FTIR-ATR) were used to examine the nanofibers' morphology and chemical characteristics. Water contact angle and water vapor transmission rate of dressings were measured. When the thymol concentration of the dressing was increased, the wettability of the dressing decreased by an average of 54%. The dressings' antimicrobial activity was determined using the colony count method, which dressings effectively inhibited the development of *E. coli* and *S. aureus*. Furthermore, cell attachment, cell viability, and in vitro cytotoxicity experiments have demonstrated the biocompatibility and cytocompatibility of the dressings, as well as their suitability for MSCs attachment. Altogether, the produced dressing was shown to have immense potential as a wound dressing.

**Keywords:** Wound dressing; Electrospinning; Thymol; Human Amniotic Membrane, Antibacterial agent.

### 1. Introduction

As our body's primary immunological barrier, skin protects us from microorganism infiltration and dehydration [1]. Thus, the major role of the skin is to shield the beneath muscles, bones, ligaments, and internal organs from exposure to external biological, chemical, mechanical, and physical agents [2]. The wound is a rupture in the tissue caused by an external laceration on the skin that results in trauma [3]. Due to the minimal tissue loss and rapid healing process associated with surgical incisions, wounds can be closed using various techniques, including adhesive strips, sutures, or

skin adhesives (closure by primary intention), unless an underlying pathological circumstance impairs the healing process [4]. Any deviation from normal healing can result in chronicity or fibrosis. This divergence could result from an underlying condition that affects, for example, the blood circulation (peripheral vascular disease) or the immunological system (immunosuppression). Additionally, it may be triggered by a metabolic disease (e.g., diabetes), pharmaceutical use, or radiation therapy [5, 6]. An incorrect repair process can result in serious injuries, such as the loss of skin, infection, impairment to adjacent

tissues and even systemic tissues [7]. As a result, it is critical to produce wound dressings capable of preventing germs from penetrating the wound and microorganisms from growing.

Since 1980, topological solutions such as membranes/sponges [8], hydrogels [9], films [10], nanogel/microgel [11], scaffolds/bandages [12], and nano/micro-fibers [13] have been studied. Among them, nano/micro-fibers exhibit desirable wound dressing qualities such as exudate absorption, oxygen permeability, high surface area, and antibacterial capabilities, largely ascribed to nanotechnology's evolution [3, 14].

Nanofibrous dressings typically have a larger porosity, allowing for greater water and oxygen permeability, improved nutrition exchange, and the elimination of metabolic waste products [15]. Additionally, nanoscale fibers can aid in hemostasis by providing small dressing interstitial spaces and a large surface area. Not only can the small hole size of nanofibrous dressings protect the wound from bacterial infection and cell/tissue ingrowth, but nanofibrous dressings can also provide good conformability, resulting in enhanced coverage and infection prevention [6, 16].

Bombyx Mori (silkworm) silk is a naturally renewable resource composed primarily of two types of proteins called Fibroin and Sericin [17, 18]. Silk fibroin (SF) has several unique properties that make it an attractive material for clothing, drug delivery, scanning, and tissue engineering. Additionally, it is a substance that has been approved by the Food and Drug Administration (FDA) for some biomedical applications [19]. SF dressings contain advantageous attributes, including delayed degradation, abundant supply, low immunogenicity, high water absorption capacity, hemostatic capabilities, superior air permeability, and inexpensive cost. Additionally, SF is a highly flexible polymer with outstanding mechanical qualities, including tensile strength (0.5 GPa), breaking elongation (15%), and elasticity (<35%) [20, 21]. SF promotes wound healing by increasing the adhesion, distribution, and proliferation of epidermal and fibroblast cells on scaffolds. SF is a versatile material that can be produced in various forms [22].

The amniotic membrane (AM) is the placenta's innermost layer (about 0.02–0.5 mm thick) that comes in direct contact with the amniotic fluid, acting as a metabolic filter and a supply of cytokines and growth factors for the fetus [23]. Additionally, AM stem cells have distinct anti-inflammatory, fibrosis, scarring, and antibacterial properties, as well as minimal immunogenicity, angiogenesis stimulation, and oxidative stress inhibition [24, 25]. It has been widely utilized to treat a variety of acute and chronic diseases, surgery reconstructing,

dentistry, urology, oncology, and otolaryngology, as well as diabetic neurovascular ulcers and different kinds of postsurgical and post-traumatic wounds openings. Specific applications present challenges due to mechanical durability, donor variability, and membrane properties associated with the preservation approach [26]. Lyophilization is one of the safest techniques for clinical usage, with the advantages of keeping the ultrastructure, facilitating and expense storage, and transportation, which enables the use of AM in diverse body sites and for extended periods [23, 24, 26].

The growth of bacterial resistance due to antibiotic overuse and the possible danger of nanoscale antimicrobial particles have sparked widespread public concern about their long-term safety. Due to their safety and comprehensive antibacterial protection, natural antibacterial components derived from plants have become interesting options [27]. Thymol (THY), a naturally occurring phenol chemical with a white aromatic crystalline form, is the primary constituent of the essential oils obtained from *Lippia gracilis* and possesses various biological properties, including antimicrobial, antioxidant, antinociceptive, local anesthetic, and anti-inflammatory properties [28]. Thymol has a tremendous potential to replace commonly used antibiotics with no microbial drug resistance due to its broad-spectrum antibacterial activity. Additionally, the United States Food and Drug Administration (FDA) has accepted Thymol as a safe substance [29]. Regrettably, most naturally produced medications are unstable in biological environments, have limited water solubility, and exhibit poor delivery to target areas [30]. Nowadays, medication delivery techniques have been created to circumvent these constraints. Electrospinning, as a simple and low-cost fabrication technique, has the ability to produce fibers with micro/nano dimensions to mimic the native structure of ECM [31]. Recently, biocompatible Manuka honey/SF fibrous matrices were fabricated by electrospinning of aqueous PEO solution as wound dressing materials. In this study, in-vivo wound healing assay indicates that the prepared Manuka honey/SF fibrous matrices demonstrated excellent biocompatibility and enhanced wound healing process [32]. Guldmeter et al. prepared nanofiber webs based on olive leaf extract loaded SF/hyaluronic acid for wound dressing applications. The cytotoxicity of prepared nanofiber webs was evaluated in-vitro against the human epidermal keratinocytes cells. These results suggested that the developed electrospun nanofibers were nontoxic and suitable candidates for wound dressing material [33]. Shadai et al. developed starch nanoparticles as a vitamin E-TPGS carrier loaded in SF/PVA/Aloe vera nanofibrous by electrospinning tech-

nique. These results indicated that the prepared nanofibrous dressing of SF/PVA/Aloe vera containing 5% Vitamin-E-loaded starch NPs can be a potential dressing for treating skin wounds [34]. Electrospun nanofibers have the potential to be a promising drug carrier for thymol, enhancing its bioactivity, achieving prolonged drug release, and minimizing the toxicity associated with overdosage [29].

This study aimed to fabricate a new bioactive by-layer wound dressing that could deliver thymol to the wound area as a natural antibacterial agent using the human amniotic membrane and silk fibroin. The dressings' structure, morphology, and physicochemical properties were investigated and measured. The biodegradability, biocompatibility, and cytotoxicity of wound dressing were all evaluated. Antimicrobial activity was measured in order to assess the bacteria's susceptibility. All data indicate that this study leads to the creation of a novel and unique dressing containing SF biopolymer nanofibers and decellularized human amniotic membrane along with thymol by electrospinning technique, which is capable of achieving wound healing needs.

## 2. Material and Methods

### 2.1. Materials

Children's Medical Center, Iran graciously donated decellularized human amniotic membrane (dehAM). *Bombyx mori* silkworm cocoons were obtained from the Guilan agricultural organization in Iran. Lithium Bromide (LiBr), Sodium Carbonate anhydrous ( $\text{Na}_2\text{CO}_3$ ), Thymol, cellulose dialysis tubes (12 KDa, 12400 MWCO), Formic Acid, Absolute Ethanol (99.7%), Glutaraldehyde (40%), Dimethyl sulfoxide (DMSO), Mueller Hinton Agar (MHA), 3-(4,5-Dimethylthiazol-2-yl)-2,5-diphenyltetrazolium bromide (MTT), and other materials used in biological protocols, including trypsin, Phosphate-buffered saline (PBS), fetal bovine serum (FBS), and Dulbecco's Modified Eagle's Medium (DMEM) were purchased from Sigma-Aldrich China Inc. Mesenchymal stem cells were provided by Research Center for Advanced Technologies, Tehran Heart Center, Iran. Microorganisms including *Staphylococcus Aureus* (ATCC29212) and *Escherichia coli* (ATCC25922) were also provided from Pasteur institute. Throughout the experiment, ultrapure water was used. All compounds utilized in this study were analytical grade and were not further purified.

### 2.2. Extraction of Silk Fibroin

SF was prepared using the method described in the literature [35]. Briefly, cocoons were boiled in a 0.02M  $\text{Na}_2\text{CO}_3$  aqueous solution at 100°C for 45 min, and then Sericin was removed by rinsing three

times with ultrapure water at 100°C for 10 min. The degummed silk was dissolved in 9.3 M Lithium bromide (LiBr) solution at 60°C for 4 hours and samples were dialyzed against ultrapure water with changes at regular time points, then centrifuged (PIT-premium 20000R, Iran) in 9000 rpm at 4°C for 15 minutes, lyophilized (Pishtaz Engineering F0-6, Iran) and stored at room temperature until further use.

### 2.3. Fabrication of Electrospun dehAM /SF mat containing Thymol

According to the results of experimental trial, a solution of 13% wt/v silk fibroin in Formic acid was made. Following that, three solutions containing 5% wt/wt, 10%wt/wt and 15% wt/wt thymol were prepared; the solutions were then put into syringes fitted with a 22 G stainless steel needle for electrospinning (NanoAzma, Iran). On the collector, dehAM (55 cm<sup>2</sup>) was deposited. The voltage, feeding rate, and distance between the tip and the collector were set to 20 kV, 0.2 mL h<sup>-1</sup>, and 15 cm, respectively. Figure 1 depicts schematic of the fabrication process. SF nanofibers were electrospun on the dehAM as a control group. The mats were submerged in ethanol for 10 minutes to convert the amorphous phase of SF to an insoluble  $\beta$ -sheet and increase SF water stability. Table 1. summarizes the compositions of each group.

### 2.4. Characterization of Electrospun dehAM/SF/THY mat

#### 2.4.1. Scanning Electron Microscopy (SEM)

SEM (SERON Technology, AIS-2100, Korea) was used to analyze the morphology of nanofibers. The average diameters of the nanofibers were determined using ImageJ software by measuring the average value of 50 nanofibers in the SEM images.

#### 2.4.2. Fourier transform infrared spectroscopy – attenuated total reflectance (FTIR-ATR)

FTIR-ATR spectroscopy (PerkinElmer, USA) was used to investigate pure Silk Fibroin and dehAM/SF/THY mats, separately.

#### 2.4.3. Contact angle measurement

The wettability of a wound dressing material is one of the most critical surface qualities that impact its biological function. Water contact angle measurements were taken on fibrous membranes to estimate their surface wettability using a Surface Tension Meter (OPTICS Z5, Iran). Each membrane sample received 3  $\mu\text{L}$  of deionized water, and each sample was analyzed in triplets.

#### 2.4.4. Water Vapor Transition rate (WVTR)

Water vapor transmission rates (WVTR) were

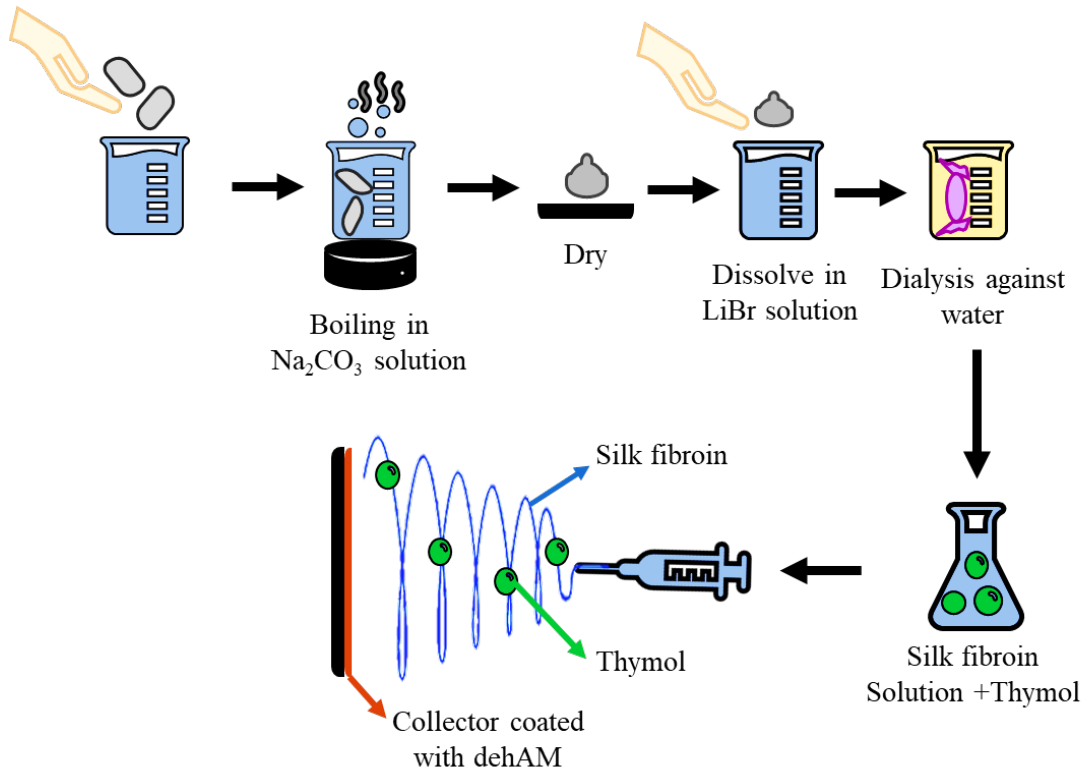


Fig. 1- schematic of the fabrication process.

Table 1- Composition of each group

	SF (wt%)	THY (wt/wt%)
dehAM/SF	13	-
dehAM/SF/T5	13	5
dehAM/SF/T10	13	10
dehAM/SF/T15	13	15

determined using the ASTM E96 standard test procedure. A cylindrical glass container with a 1.5 cm<sup>2</sup> surface area was supplied with 50 mL deionized water and sealed at the top with the dressing. The bottle was placed in the environmental chamber at 37°C and relative humidity of 40%. The assembly's weight was observed at regular intervals of one hour for 24 hours, and the WVTR was measured by the slope of the graph using a linear function by the equation 1[36]:

$$\text{WVTR} = \frac{\text{weight loss}}{A} \text{ (g/m}^2\text{day)} \quad (1)$$

#### 2.4.5. Thymol release study

The dressings (with a total weight of 5 mg) were soaked in 2 mL of PBS adjusted to a pH of 7. The specimens were then incubated at 37°C in an incubator shaker under rotation (60 rpm) to simulate physiological function. The samples were centrifuged at various time points, and the supernatant (1 mL) absorbance at 274 nm was determined to compute the amount of thymol released. Thymol solutions containing 0.2–2% wt/v thymol in Formic acid were generated to calculate the calibration curve, and their UV absorptions at 274 nm were recorded. All experiments were repeated three times.

#### 2.4.6. Degradation assessment

The dressings were incubated in a 1.5 mL solution of PBS for 7, 14, and 21 days at 37°C, pH 7. (60 rpm). Dressings were freeze-dried and weighed at various intervals. The degradation at each time was estimated using the following equation [37]:

$$\text{Weight loss (\%)} = \frac{W_i - W_t}{W_t} \times 100 \quad (2)$$

Where  $W_i$  is the initial weight of the sample and  $W_t$  the weight of the sample at time  $t$ .

#### 2.4.7. Cell culture

MSC cells were grown at 37°C in a 5% CO<sub>2</sub> atmosphere in DMEM media supplemented with 10% FBS and 1% penicillin/streptomycin. The dressings were trimmed to the proper size and sterilized by soaking them in 70% ethanol filtered through a 0.22-micron filter and rinsed three times with PBS (15 minutes each time), followed by a 20-minute UV exposure. To examine cell adherence to the dressings, MSC cells were seeded on each dressing and incubated for 3 days at 37°C, 5% CO<sub>2</sub>. Each sample was fixed for 40 minutes at 20°C in a 2.5% glutaraldehyde solution and dehydrated for 10 minutes in gradient ethanol. SEM was used to examine cell morphology and cell adhesion.

#### 2.4.8. Cell toxicity assessment by MTT assay

Following 1, 3, and 7 days after cell seeding, the biocompatibility of the dressings was determined using 3-(4,5-dimethylthiazol-2-yl)-2,5-diphenyl tetrazolium bromide (MTT) assay. Before seeding cells, dressings were placed in 96-well plates and sterilized using the same process as the cell adhesion assay. MSC cells were seeded and incubated in a sterile environment. For 3.5 hours, the samples were incubated (T=37°C, 5% CO<sub>2</sub>) in an MTT reagent. The formazan crystals were dissolved in DMSO, and the absorbance at 570 nm was determined using an ELISA plate reader (Biotec, ELX800, USA). As a control group, a serum-free culture medium was used.

#### 2.4.9. Antibacterial assay

For two of the most commonly detected gram-negative and gram-positive bacteria found in the wound region, the bacterial inhibition was assessed using a revised AATCC-100 Testing Method [38]. In a 100 µL sterilized feeding solution, bacterial suspensions (*E. coli* and *S. aureus*) with  $1.5 \times 10^8$  colony forming units (CFU) mL<sup>-1</sup> (0.5 McFarland) were applied on 4 cm<sup>2</sup> cut samples and covered with another dressing. The dressings and suspension were shaken after a 24-hour incubation time at 37°C, and 0.1 mL of each sample was cultured on Muller Hinton agar medium. After another 24 hours of incubation at 37°C, the colonies were counted.

#### 2.4.10. Statistical analysis

One-way analysis of variance (ANOVA) followed by Tukey's post hoc test was used to analyze the results.

### 3. Results and Discussion

#### 3.1. SEM analysis

Figure 2 depicts the morphology of nanofibers and size distribution. The diameter analyses indicated that dehAM/SF has an average diameter of 260±58 nm, which decreases when thymol is added, from 126±31 nm in dehAM/SF/T5 to 104±21 nm in dehAM/SF/T10. This could be related to thymol's plasticizing properties and the rearranging of polymer chains, which resulted in a drop in the viscosity of the polymer solution. The addition of 15%w/w thymol to the electrospinning solution increased the average diameter of dehAM/SF/T15 to 189±46 nm, which may be owing to the thymol's low solubility in the solution. Furthermore, the diameter of the nanofibers is comparable to that of the collagen fibrils found in the ECM (50-500 nm), indicating the dressings' ability to replicate the properties of native tissue and create an optimal environment for cell migration, adhesion, and proliferation.

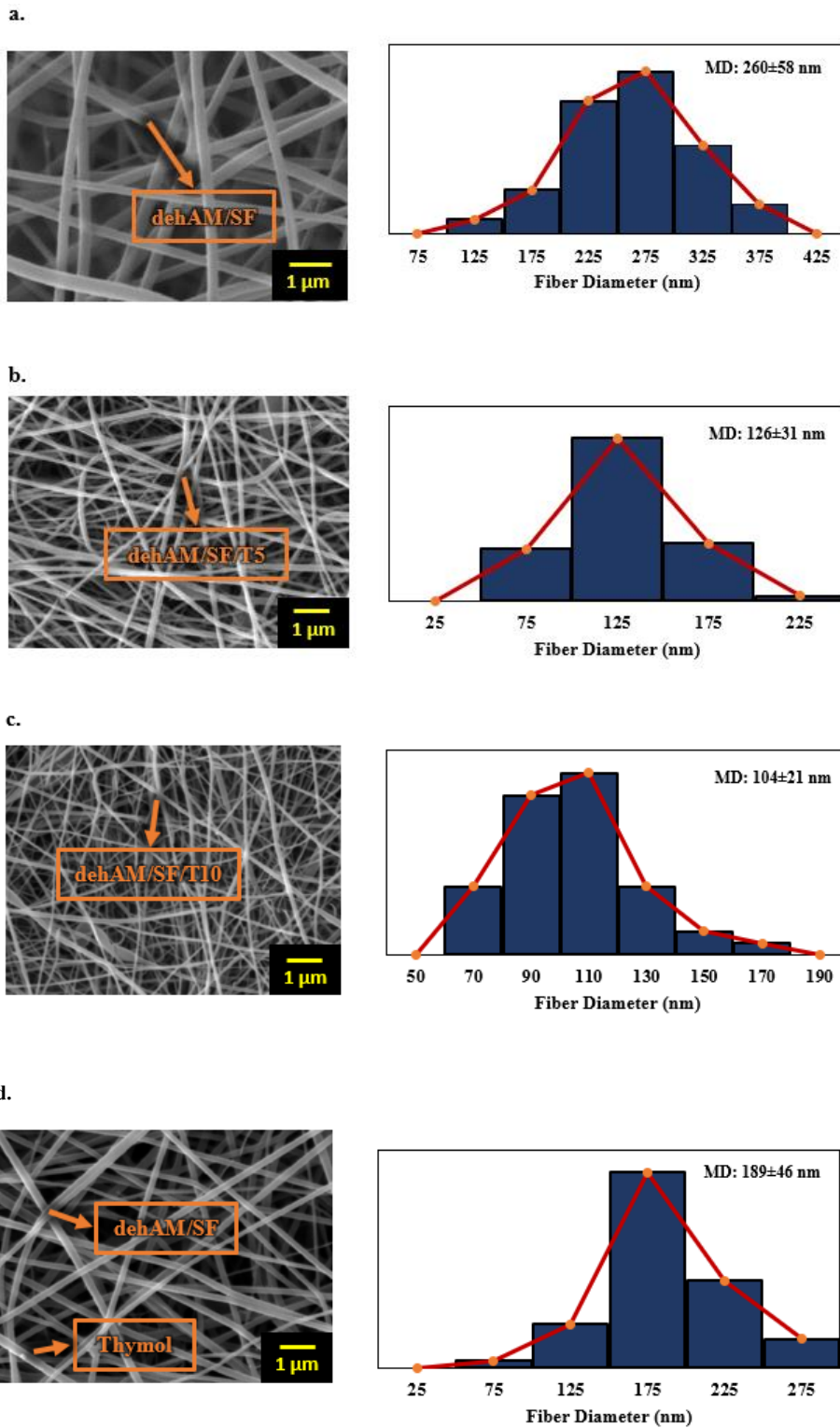


Fig. 2- SEM images and diameter distributions of nanofibers a. deHAM/SF b. deHAM/SF/T5 c. deHAM/SF/T10 d. deHAM/SF/T15.

### 3.2. FTIR-ATR results

Figure 3. shows the chemical bonding existing in the produced wound dressings. It can be observed from figure 3.a that the presence of peaks at  $1650\text{ cm}^{-1}$  and  $1526\text{ cm}^{-1}$  are due to the amide I and amide II of SF. These peaks have shifted to  $1624\text{ cm}^{-1}$  and  $1514\text{ cm}^{-1}$  as a result of formation of  $\beta$ -sheets from random coils which proves the accuracy of the SF cross-linking process. Additional bondings were found, including OH<sup>-</sup> at  $3282\text{ cm}^{-1}$ , CH<sup>2</sup> at  $2980\text{ cm}^{-1}$ ,

asymmetric C-O-C at  $1239\text{ cm}^{-1}$ , and symmetric C-O-C at  $1169\text{ cm}^{-1}$ , which are identical in both as-synthesized and cross-link specimens. Table 2. summarizes the wavenumber of corresponding bonds. In figure 3.b a peak at  $671\text{ cm}^{-1}$  was seen when thymol was added to the fabricated wound dressing, matching aromatic C-H bonding. Additionally, thymol possesses an OH-group, phenolic bond at  $3289\text{ cm}^{-1}$  that overlaps with the OH<sup>-</sup> bond in SF, resulting in a slightly stronger peak.

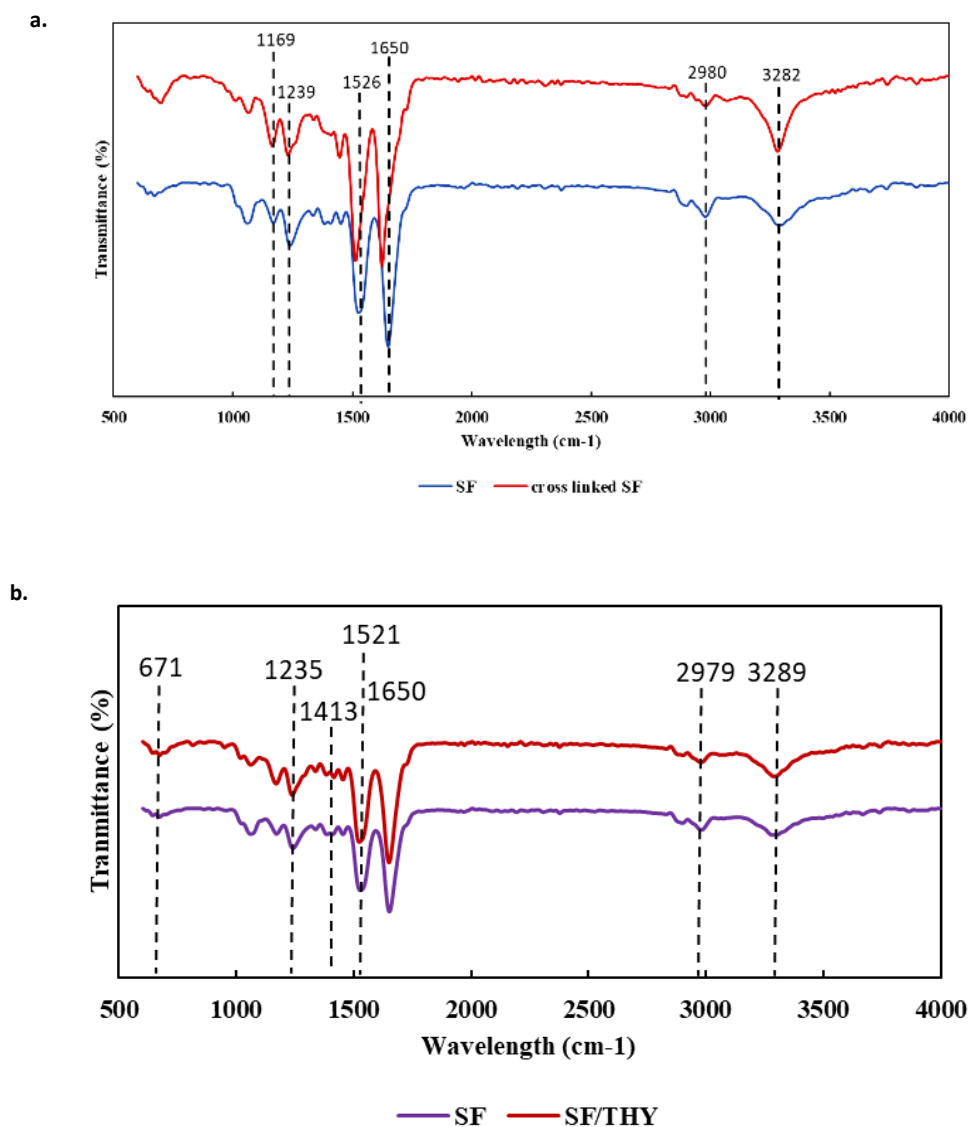


Fig. 3- FTIR-ATR spectrograph of a. the effect of cross linking on Silk Fibroin b. SF and SF/T15.

### 3.3. Contact angle results

The presence of polar functional groups reduces contact angles by increasing surface energy. These functional groups enable binding to water molecules and extracellular matrix proteins, creating favorable sites for cell attachment. In contrast, surfaces with nonpolar chemical compositions minimize protein adsorption and cell adhesion [39]. Wettability was determined for all dressings as well as SF nanofibers to observe the impact of dehAM on the hydrophilic nature of wound dressings. Generally, the moist atmosphere within the wound dressing would promote cell adhesion and cell growth. The

contact angle measures are depicted in figure 4. As demonstrated, the SF nanofibers have an average contact angle of  $86.6 \pm 4.6^\circ$ , which is believed to be a hydrophobic wound dressing, however, adding a thin coating of dehAM increased the wettability greatly to  $24.5 \pm 3.2^\circ$ , which could be owing to the polar groups present in dehAM [32, 33]. Additionally, figures regarding to dehAM/SF/T5, dehAM/SF/T10 and dehAM/SF/T15 illustrate the effect of various thymol concentrations. When the thymol concentration of the dressings was increased, the wettability of the dressings decreased.

Table 2- Wavenumber of corresponding bonds

Peak (1/cm)	Bond
1650	Amide I of SF
1526	Amide II of SF
1624	$\beta$ -sheets
1514	$\beta$ -sheets
3282	OH
2980	CH <sup>2</sup>
1239	Asymmetric C-O-C
1169	Symmetric C-O-C
671	Aromatic C-H
3289	Phenolic bond

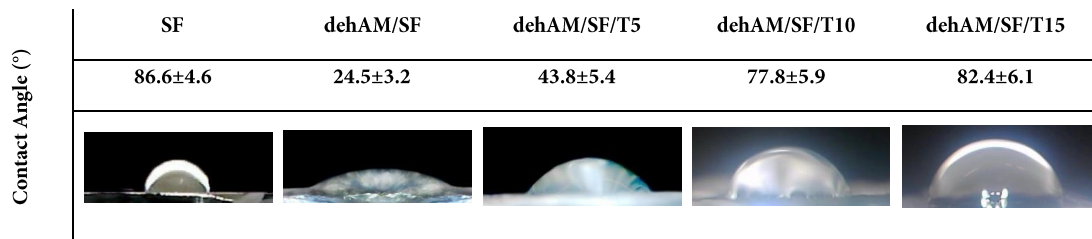


Fig. 4- Contact angle of the dressings.

### 3.4. WVTR results

To prevent dehydration and exudate accumulation in the wound and to stimulate tissue regeneration, a suitable wound dressing material should be permeable to water vapor. Gas permeation through a thin membrane is frequently separated into two stages: dissolution of gas molecules within the membrane and transmission across the membrane. Thus, the permeability of a polymeric film to water vapor is dependent on various parameters, including the presence of pores in the membrane, its degree of hydrophilicity, the polymer crystalline phase, and its molecular mobility [35]. The results suggest that increasing the thymol content in the dressings decreased the water vapor transfer rate from  $7130 \pm 79$  g/m<sup>2</sup>/day and  $6285 \pm 56$  g/m<sup>2</sup>/day for dehAM/SF/T10 for dehAM/SF/T5 to  $5146 \pm 104$  g/m<sup>2</sup>/day for dehAM/SF/T15. The decreasing trend could result from the reduction in free volume and molecular mobility due to the creation of a dense network of thymol and SF via new hydrogen bonding.

### 3.5. Thymol release profile

Eight solutions ranging in concentration from  $0.2$  mg mL<sup>-1</sup> and  $2$  mg mL<sup>-1</sup> were quantified using UV-visible spectrophotometry with Formic acid serving as a blank sample at a physiological pH 7. At 274 nm, the absorbance was measured, demonstrating a linear calibration curve ( ) between absorbance and thymol concentrations.

The in vitro thymol release profiles of the dressings were investigated over two weeks at 37 °C. As illustrated in Fig. 5, the release of thymol from nanofibers was rather rapid during the first 24 hours of PBS treatment but then reduced and eventually reached its peak after two weeks. During the first 24 hours, a burst release of thymol nanoparticles (about  $11$  mg mL<sup>-1</sup>) occurs. After the initial phase, the pace of thymol release slowed to the point where the release profile became flattened. Generally, controlled drug release was obtained due to the nanofibers' benefits.

### 3.6. Degradation profile

The amount of weight reduction at various incubation durations is depicted in Figure 6. Because the dose of thymol used did not affect the degradation rate, only the dehAM/SF/T15 dressing was used in the test. The results of the degradation experiments yielded that the dressing loses 25% of its weight after 7 days, followed by 72% once the experiment is finished. According to the observation, the dressing's degradable component is primarily SF nanofibers. As a result, SF has a high resistance to dissolving, heat degradation, and enzymatic activity [20]. Therefore, hydrolysis is used to carry out the in vitro degradation. Thymol also undergoes degradation reactions such as oxidation, polymerization, disproportionation, and cyclization [28].

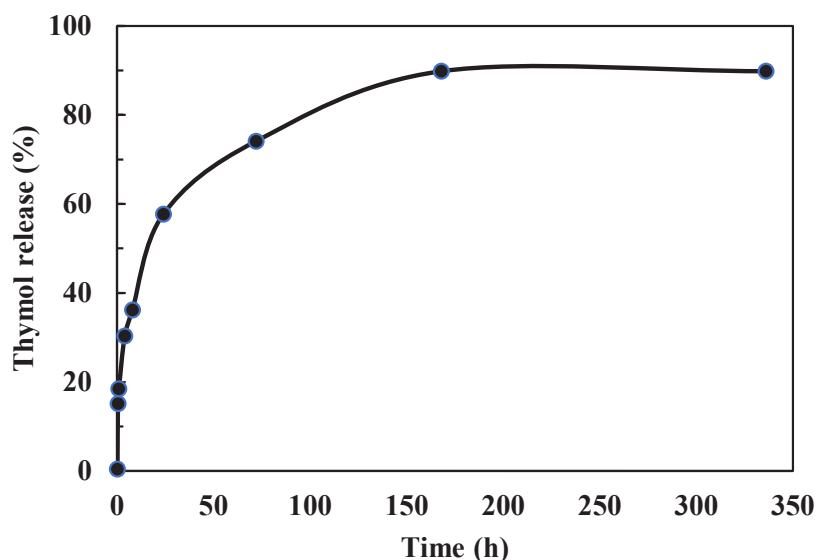


Fig. 5- Thymol release profile from dehAM/SF/T15 nanofibers after immersion in PBS.

### 3.7. Cell adhesion

Figure 7. depicts the cell adhesion, cell morphology and filopodia of Mesenchymal stem cells after 72 hours of incubation. At great magnification, we could discern the transition of the cell shape into spindles and triangles. Although all dressings provided enough surfaces for MSCs attachment, the elongation of MSCs was seen to be different as the thymol concentration of the

dressings increased. The degree of elongation and spindle-shapedness of the cells decreases from sample dehAM/SF to dehAM/SF/T15. Cells grown on the dehAM/SF/T15 dressing exhibited a more rounded shape and an inclination to cluster. Additionally, the results demonstrated that the dressings could mimic the extracellular matrix environment, which was advantageous to cell adhesion and growth.

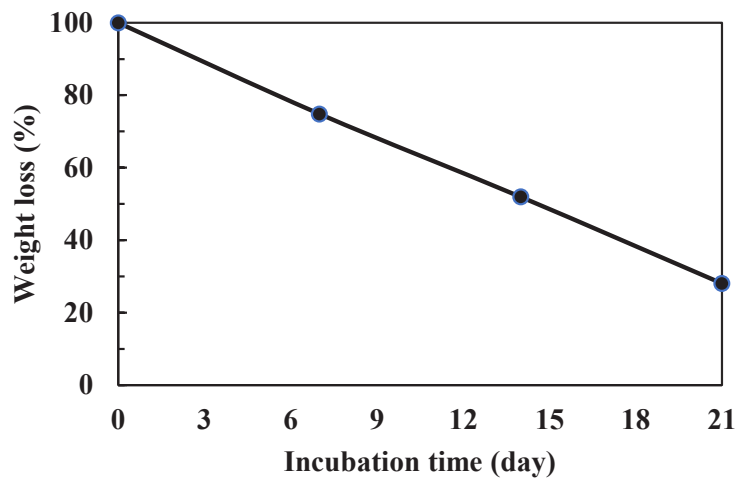


Fig. 6- Degradation profile of dressing after 7, 14 and 21 days of incubation in PBS.

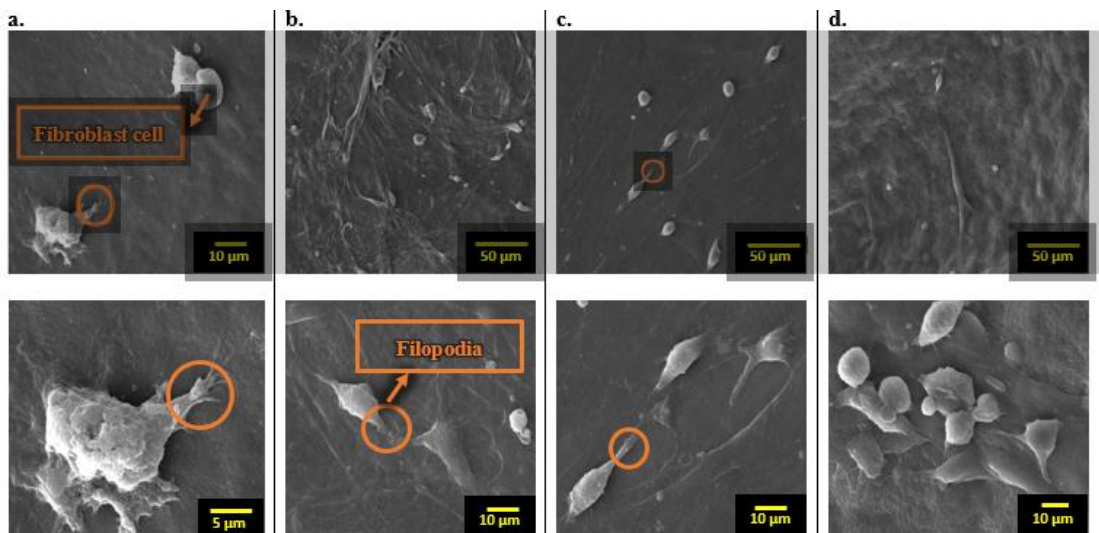


Fig. 7- SEM images of MCS cells seeded at the surface of a. dehAM/SF b. dehAM/SF/T5 c. dehAM/SF/T10 d. dehAM/SF/T15 after 72 h; Filopodia are shown with orange circles.

### 3.8. MTT assay

According to the MTT assay results provided in figure 8, the viability of MSCs on the dressings is greater than that of the control sample, implying that the addition of thymol is not toxic. Additionally, cell proliferation was aided by cytokines and growth factors in the decellularized human amniotic membrane.

### 3.9. Antibacterial assay

According to the literature [2], the most prevalent microorganisms found in infectious skin wounds are *Escherichia coli* (gram-negative) and *Staphylococcus aureus* (gram-positive). As a result, the antibacterial property of wound dressings is critical. Thymol, as a phenolic compound, penetrates the bacterial cell membrane and disrupts the structure and function of the membrane. This disruption leads to increased membrane permeability and the leakage of vital substances from the bacterial cell, ultimately causing cell death. Thymol can inhibit vital processes inside the bacterial cell, such as protein transcription and translation, thereby reducing the production of toxic substances and enzymes needed by bacteria, which inhibits bacterial growth and proliferation [42]. As illustrated in Figure 9, the antibacterial activity of the dehAM/SF/T15 dressing was determined using the dilution method towards *E. coli* and *S. aureus* (colony count). The findings indicate that the dressings are highly efficient against certain microorganisms. Additionally, the dressing had a threefold antibacterial effect against *S. aureus* compared to *E. coli*, which

could be explained by the fact that gram-negative bacteria have a more complicated and thicker cell wall composed primarily of lipopolysaccharide molecules that behave as a hydrophilic shield, preventing hydrophobic structures such as Thymol from diffusing into the cell wall [28]. In terms of thymol's antibacterial effectiveness against gram-positive bacteria, it is hypothesized that direct contact between thymol and intracellular biomacromolecules leads to DNA structural changes and bacterial mortality [29].

### 4. Conclusion

Although SF nanofibers have been extensively used as a promising biomaterial for wound healing due to its appropriate mechanical properties as well as its biocompatibility, its low wettability hinders cell processes such as cell adhesion and cell proliferation. Thus:

1. In this study, decellularized hAM was added as a solid substrate to not only promote cell adhesion and cell migration but also improve cell proliferation due to the presence of growth factors and cytokines necessary for wound healing.
2. Thymol was also incorporated into SF nanofibers via electrospinning as a natural antibacterial agent to protect the wound area against common microorganisms.
3. In summary, this study confirmed that thymol-loaded dehAM/SF dressing fabricated via electrospinning technique is a proper candidate for wound healing by preventing infections and healing acceleration effect.

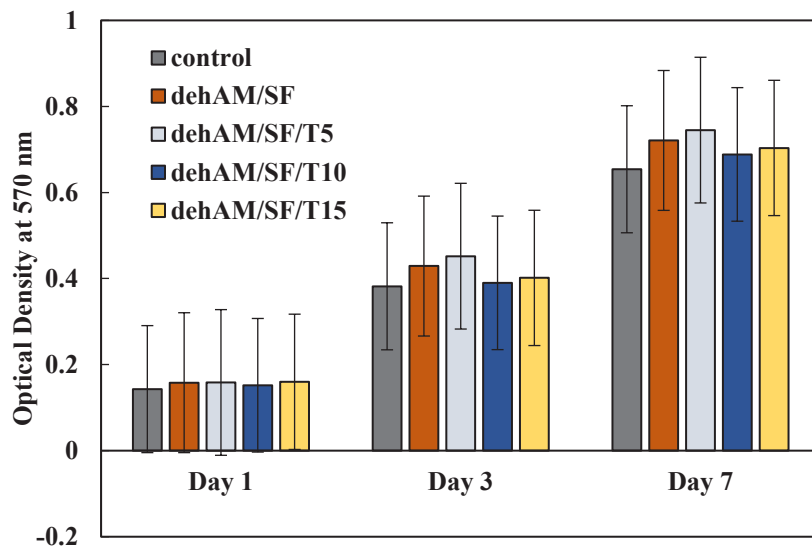


Fig. 8- Cytotoxic effects of nanofibrous dressings on MCS cells during a period of 1, 3 and 7 days based on the MTT assay (P-value <0.05).

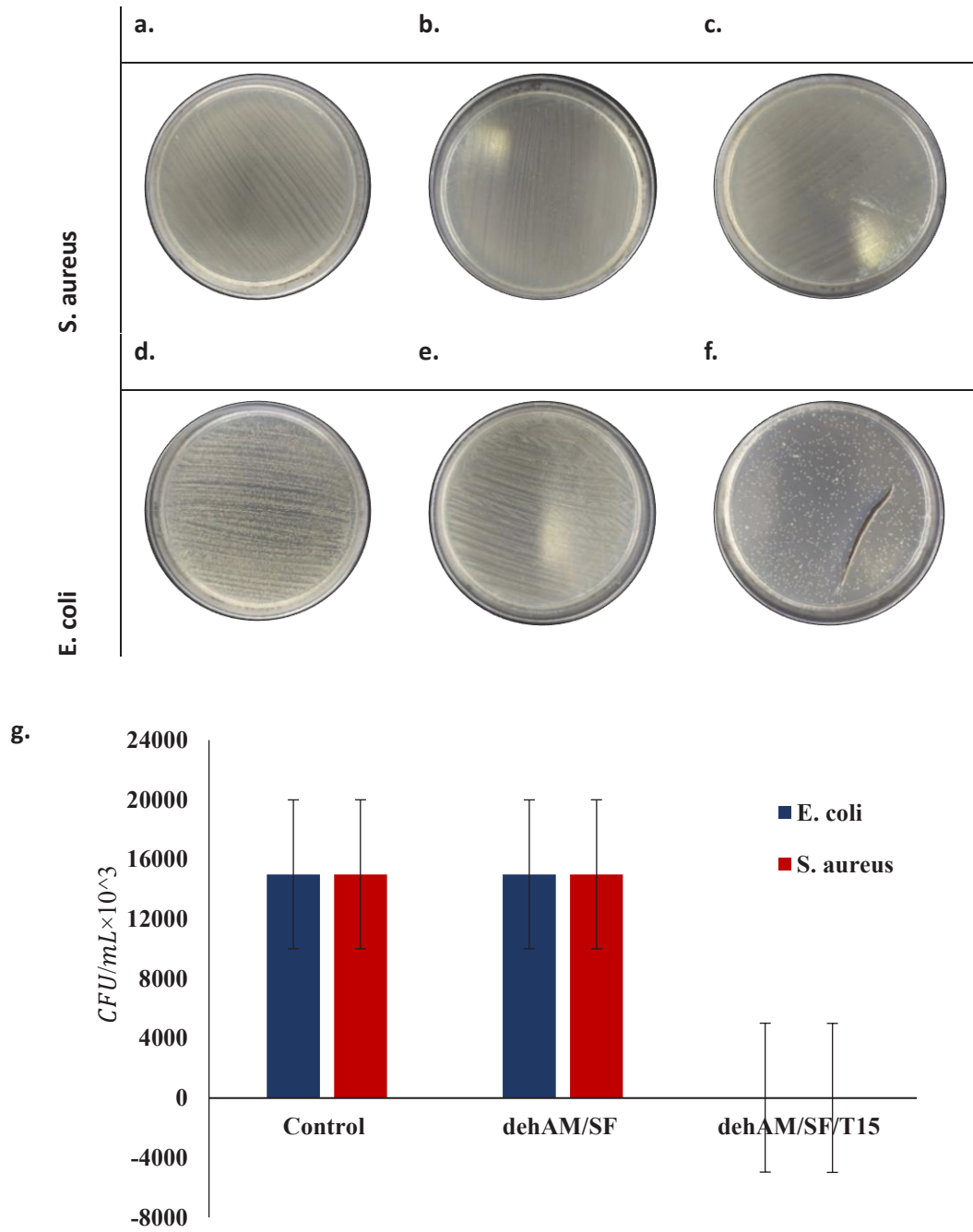


Fig. 9- Antibacterial test Petri dishes of a. negative control, b dehAM/SF c. dehAM/SF/T15 d. positive control e. dehAM/SF f. dehAM/SF/T15 from their bacterial solution against *E. coli* and *S. aureus*. g. Antibacterial efficacy of nanofibrous mats after exposure to *E. coli* and *S. aureus*.

## References

1. M. F. P. Graça, S. P. Miguel, C. S. D. Cabral, and I. J. Correia, "Hyaluronic acid-Based wound dressings: A review," *Carbohydr. Polym.*, vol. 241, 2020.
2. D. Simões, S. P. Miguel, M. P. Ribeiro, P. Coutinho, A. G. Mendonça, and I. J. Correia, "Recent advances on antimicrobial wound dressing: A review," *Eur. J. Pharm. Biopharm.*, vol. 127, no. December 2017, pp. 130–141, 2018.
3. R. Ambekar, B. K.-E. P. Journal, and undefined 2019, "Advancements in nanofibers for wound dressing: A review," Elsevier.
4. A. Gupta, M. Kowalczyk, W. Heaselgrave, S. T. Britland, C. Martin, and I. Radecka, "The production and application of hydrogels for wound management: A review," *Eur. Polym. J.*, vol. 111, no. November 2018, pp. 134–151, 2019.
5. G. Han and R. Ceilley, "Chronic Wound Healing: A Review of Current Management and Treatments," *Adv. Ther.*, vol. 34, no. 3, pp. 599–610, Mar. 2017.
6. S. Homaeigohar and A. R. Boccaccini, "Antibacterial biohybrid nanofibers for wound dressings," *Acta Biomater.*, vol. 107, no. 2020, pp. 25–49, 2020.
7. I. Negut, V. Grumezescu, and A. M. Grumezescu, "Treatment strategies for infected wounds," *Molecules*, vol. 23, no. 9, pp. 1–23, 2018.
8. A. Davis, K. B.-D. S. Journal, and undefined 2016, "Bioactive Hybrid Composite Membrane with Enhanced Antimicrobial Properties for Biomedical Applications," search.ebscohost.com.
9. G. Sun, X. Zhang, Y. Shen, ... R. S.-P. of the, and undefined 2011, "Dextran hydrogel scaffolds enhance angiogenic responses and promote complete skin regeneration during burn wound healing," *Natl. Acad. Sci.*
10. D. Altiok, E. Altiok, F. T.-J. of M. S. Materials, and undefined 2010, "Physical, antibacterial and antioxidant properties of chitosan films incorporated with thyme oil for potential wound healing applications," *Springer*, vol. 21, no. 7, pp. 2227–2236, Jul. 2010.
11. S. Anjum, A. Sharma, M. Tummalapalli, J. Joy, S. Bhan, and B. Gupta, "A novel route for the preparation of silver loaded polyvinyl alcohol nanogels for wound care systems," *Int. J. Polym. Mater. Polym. Biomater.*, vol. 64, no. 17, pp. 894–905, Dec. 2015.
12. S. Kumar et al., "Development of novel chitin/nanosilver composite scaffolds for wound dressing applications," *Springer*, vol. 21, no. 2, pp. 807–813, Feb. 2009.
13. A. E. Purushothaman, K. Thakur, and B. Kandasubramanian, "Development of highly porous, Electrostatic force assisted nanofiber fabrication for biological applications," *Int. J. Polym. Mater. Polym. Biomater.*, vol. 69, no. 8, pp. 477–504, May 2020.
14. R. Yadav, K. B.-E. of Nanobiomaterials, and undefined 2016, "Bioabsorbable engineered nanobiomaterials for antibacterial therapy," Elsevier.
15. V. Andreu, G. Mendoza, M. Arruebo, and S. Irusta, "Smart Dressings Based on Nanostructured Fibers Containing Natural Origin Antimicrobial, Anti-Inflammatory, and Regenerative Compounds," *Mater.* 2015, Vol. 8, Pages 5154–5193, vol. 8, no. 8, pp. 5154–5193, Aug. 2015.
16. P. Zahedi, I. Rezaei, S. O. Ranaei-Siadat, S. H. Jafari, and P. Supaphol, "A review on wound dressings with an emphasis on electrospun nanofibrous polymeric bandages," *Polym. Adv. Technol.*, vol. 21, no. 2, pp. 77–95, Feb. 2010.
17. Z. Liu, S. Shang, K. Lok Chiu, S. Jiang, and F. Dai, "Fabrication of silk fibroin/poly(lactic-co-glycolic acid)/graphene oxide microfiber mat via electrospinning for protective fabric," *Mater. Sci. Eng. C*, vol. 107, no. October 2019, p. 110308, 2020.
18. P. P. Patil, M. R. Reagan, and R. A. Bohara, "Silk fibroin and silk-based biomaterial derivatives for ideal wound dressings," *Int. J. Biol. Macromol.*, 2020.
19. M. Pollini, "Bioinspired Materials for Wound Healing Application: The Potential of Silk Fibroin," 2020.
20. M. Farokhi, F. Mottaghtalab, Y. Fatahi, A. Khademhosseini, and D. L. Kaplan, "Overview of Silk Fibroin Use in Wound Dressings," *Trends Biotechnol.*, vol. 36, no. 9, pp. 907–922, 2018.
21. D. Chouhan and B. B. Mandal, "Silk Biomaterials in Wound Healing and Skin Regeneration Therapeutics: from Bench to Bedside," *Acta Biomater.*, 2019.
22. M. Ghanbari, R. Karimian, and B. Mehramouz, "International Journal of Biological Macromolecules Preparation of biocompatible and biodegradable silk fibroin / chitin / silver nanoparticles 3D scaffolds as a bandage for antimicrobial wound dressing," vol. 114, pp. 961–971, 2018.
23. A. Rodella, M. Pozzobon, M. Rigon, C. Franchin, and G. Arrigoni, "Topical application of lyophilized and powdered human amniotic membrane promotes diabetic ulcer healing," *Wound Med.*, vol. 27, no. 1, p. 100171, 2019.
24. A. Rezaei, A. Ali, M. Amir, and M. Mollapour, "Update review on five top clinical applications of human amniotic membrane in regenerative medicine," *Placenta*, vol. 103, no. September 2020, pp. 104–119, 2021.
25. S. V. Murphy et al., "Amnion membrane hydrogel and amnion membrane powder accelerate wound healing in a full thickness porcine skin wound model," *Stem Cells Transl. Med.*, vol. 9, no. 1, pp. 80–92, Jan. 2020.
26. L. Sara et al., "Human Amniotic Membrane: A review on tissue engineering, application, and storage," no. November, pp. 1–18, 2020.
27. A. Marchese et al., "Antibacterial and antifungal activities of thymol: a brief review of the literature," *FOOD Chem.*, 2016.
28. S. P. Miguel, D. Simões, A. F. Moreira, S. Rosa, and I. J. Correia, "Production and characterization of electrospun silk fibroin based asymmetric membranes for wound dressing applications," *Int. J. Biol. Macromol.*, 2018.
29. R. Najafloo, M. Behyari, R. Imani, and S. Nour, "A Mini-review of Thymol Incorporated Materials: Applications in Antibacterial Wound Dressing," *J. Drug Deliv. Sci. Technol.*, p. 101904, 2020.
30. Y. Chen, Y. Qiu, W. Chen, and Q. Wei, "Materials Science & Engineering C Electrospun thymol-loaded porous cellulose acetate fibers with potential biomedical applications," *Mater. Sci. Eng. C*, vol. 109, no. December 2019, p. 110536, 2020.
31. G. Hong, J. Yeo, M. Yang, G. H., & Kim, "Cell-electrospinning and its application for tissue engineering," *Int. J. Mol. Sci.*, vol. 20, 2019.
32. H. Yang, X. Fan, L. Ma, L. Wang, Y. Lin, S. Yu, F., ... & Wang, "Green electrospun Manuka honey/silk fibroin fibrous matrices as potential wound dressing," *Mater. Des.*, vol. 119, pp. 76–84, 2017.
33. A. Basal, G. Tetik, G. D., Kurkcu, G., BAYRAKTAR, O., Gurhan, I. D., & Atabey, "olive leaf extract loaded silk fibroin/hyaluronic acid nanofiber webs for wound dressing applications," *Dig. J. Nanomater. Biostructures*, vol. 11, 2016.
34. B. Kheradvar, S. A., Nourmohammadi, J., Tabesh, H., & Bagheri, "Starch nanoparticle as a vitamin E-TPGS carrier loaded in silk fibroin-poly (vinyl alcohol)-Aloe vera nanofibrous dressing," *Colloids Surfaces B Biointerfaces*, vol. 166, pp. 9–16, 2018.
35. D. Rockwood, R. Preda, T. Yücel, X. W.-N. protocols, and undefined 2011, "Materials fabrication from Bombyx mori silk fibroin," nature.com.
36. R. H. Pan, Z., Bora, M., Gee, R., & Dauskardt, "Water vapor transmission rate measurement for moisture barriers using infrared imaging," *Mater. Chem. Phys.*, vol. 308, 2023.
37. G. Sen, S., Das, C., Ghosh, N. N., Baildya, N., Bhattacharya, S., Khan, M. A., ... & Biswas, "Is degradation of dyes even possible without using photocatalysts?—a detailed comparative study," *RSC Adv.*, vol. 12, 2022.
38. M. Zafari et al., "Physical and biological properties of blend-electrospun polycaprolactone/chitosan-based wound dressings loaded with N-decyl-N, N-dimethyl-1-decanaminium chloride: An in vitro and in vivo study," *J. Biomed. Mater. Res. - Part B Appl. Biomater.*, vol. 108, no. 8, pp. 3084–3098, 2020.
39. X. Yu, B., He, C., Wang, W., Ren, Y., Yang, J., Guo, S., ... & Shi, "Asymmetric wetttable composite wound dressing prepared by electrospinning with bioinspired micropatterning enhances

diabetic wound healing," *ACS Appl. Bio Mater.*, vol. 3, 2020.

40. D. Yang, Z. Fang, R. Kang, K. L.-M. & Design, and undefined 2021, "Composite electrospun scaffold containing decellularized amniotic matrix for pelvic organ prolapse," Elsevier.

41. A. Ghaee, M. Karimi, ... M. L.-S.-M. S. and, and undefined 2019, "Preparation of hydrophilic polycaprolactone/modified

ZIF-8 nanofibers as a wound dressing using hydrophilic surface modifying macromolecules," Elsevier.

42. M. Y. Hajibonabi, A., Yekani, M., Sharifi, S., Nahad, J. S., Dizaj, S. M., & Memar, "Antimicrobial activity of nanoformulations of carvacrol and thymol: New trend and applications," *OpenNano*, vol. 13, 2023.